Journal of Geometry and Physics 123 (2018) 173–183

Contents lists available at ScienceDirect

Journal of Geometry and Physics

journal homepage: www.elsevier.com/locate/geomphys

Hyperbolic Shirts fit a 4-body problem

Connor Jackman [a,*], Josué Meléndez [b,1]

[a] Mathematics Department, University of California, 4111 McHenry Santa Cruz, CA 95064, USA
[b] Departamento de Matemáticas, Universidad Autónoma Metropolitana - Iztapalapa, San Rafael Atlixco 186, Col. Vicentina, CP 09340 México City, Mexico

ARTICLE INFO

Article history:
Received 11 July 2017
Accepted 15 September 2017
Available online 28 September 2017

Keywords:
Curvature computations
N-body problems
Hyperbolic dynamics

ABSTRACT

Consider the equal mass planar 4-body problem with a potential corresponding to an inverse *cube* force. The Jacobi–Maupertuis principle reparametrizes the dynamics as geodesics of a certain metric. We compute the curvature of this metric in the reduced space on the collinear and parallelogram invariant surfaces and observe some dynamical consequences.

1. Introduction

The classical *N*-body problem concerns the motions of *N* point masses subject to an attractive force proportional to the inverse square of the relative distances between the masses. Poincaré noticed in [1] (see as well [2]) that variational methods work better for 'strong forces' meaning proportional to the inverse cube or a larger power of the relative distances, due to the fact that the action becomes infinite as one approaches collisions. Consequently, for strong force *N*-body problems it is easy to show the existence of periodic orbits by minimizing the action over almost any free homotopy class. Montgomery [3] studied the inverse cube planar problem with three equal masses using the Jacobi–Maupertuis variational principle (see Eq. (4) below) and obtained uniqueness results leading to some symbolic dynamics. Recently research on this subject has been a topic of increasing interest, see for instance [3–6]. Here we examine this approach for the restricted problems of 4-bodies in a collinear configuration or 4-bodies in a parallelogram configuration. Chen in [7] observed that the shape space for 4-bodies in a parallelogram configuration (Fig. 1) is, like for the planar 3-body problem, a punctured sphere (see Figs. 2, 4) and used this to great advantage in finding new choreography type solutions to the Newtonian 4-body problem. Our main result on Chen's parallelogram shape space with an inverse cube potential is that almost every free homotopy class is realized uniquely up to symmetry by a periodic solution.

In this paper we consider the planar 4-body problem with an inverse cube force. For the inverse cube *N*-body problem the virial, or Lagrange Jacobi identity (Eq. (3) below) implies that bounded orbits must have zero energy, H, and constant moment of inertia, I. Conversely if $H = 0$ and $\dot{I} = 0$ at the initial time then the motion remains bounded as long as it exists. *Consequently in this paper we assume the energy is zero and the initial change in moment of inertia is zero for our 4-body problem.*

The key method in [3] was to compute the curvature of the corresponding Jacobi–Maupertuis metric and show that it is negative almost everywhere. One of us showed in [6] that this method fails for the 4-body equal mass inverse cube problem: the curvatures have mixed signs. The question then remains, can some of the methods be salvaged? Here we answer 'yes' by

* Corresponding author.
E-mail addresses: cfjackma@ucsc.edu (C. Jackman), jms@xanum.uam.mx (J. Meléndez).

[1] Josué Meléndez was partially supported by SEP-PRODEP, UAM-PTC-638, México.

https://doi.org/10.1016/j.geomphys.2017.09.006
0393-0440/

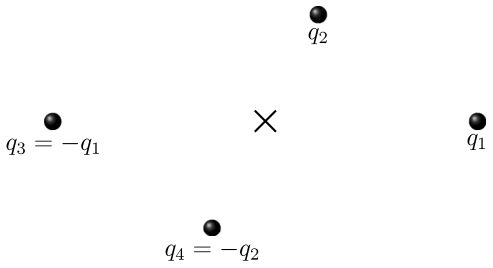

Fig. 1. A configuration of $\mathcal{P}$. Here $\times$ is the center of mass. Note there are 3 parallelogram problems in Q, each corresponding to a different choice of diagonals.

proving that there exist two invariant subproblems of this 4-body problem for which the curvatures are negative and hence methods of hyperbolic dynamics apply.

One of these subproblems is the collinear 4-body problem whose reduced configuration space we will denote by $\mathcal{C}$. The other corresponds to the parallelogram 4-body problem (see [7] and Fig. 1) whose reduced configuration space we will call $\mathcal{P}$.

It is well known that Newton's equations of motion in a potential field can be reformulated as a geodesic problem, once the total energy H is fixed. This metric on the configuration space generating the geodesics is called the Jacobi–Maupertuis metric. In our situation, due to the symmetries of Newton's equations and the special inverse cube law [8], this metric at energy zero admits a large isometry group G corresponding to translating, rotating, *and scaling* the quadrilateral formed by the 4-bodies. The metric lives on the standard configuration space for the 4-body problem, X and this quotient procedure induces a metric on the quotient space

$$Q = X/G$$

which we will also call the Jacobi–Maupertuis metric and will denote by ds^2_{JM}. Its geodesics correspond to solutions to the Marsden–Weinstein symmetry reduced Newton's equations.

In earlier work [3,6] it was shown that ds^2_{JM} is a complete metric of varying curvature on Q. Both the collinear configurations $\mathcal{C}$ and parallelogram configurations $\mathcal{P}$ sit naturally in Q. We are now able to state our main results.

Theorem 1. *The Gaussian curvature of ds^2_{JM} on both $\mathcal{C}$ and $\mathcal{P}$ is negative almost everywhere. On $\mathcal{P}$ the curvature is zero at exactly two points while on $\mathcal{C}$ the curvature is strictly negative everywhere.*

Remark. The surface $\mathcal{P}$ is topologically equivalent to a 2-sphere minus four points, or a shirt. The punctures of the 2-sphere are due to two binary collisions ($q_1 = q_3$ and $q_2 = q_4$) and two simultaneous binary collisions ($q_1 = q_4, q_2 = q_3$, and $q_1 = q_2, q_3 = q_4$). See Figs. 2, 4 for a depiction of $\mathcal{P}$.

A syzygy is a collinear configuration on the equator of $\mathcal{P}$. Note that although the masses are equal, we have four syzygy types on $\mathcal{P}$, see Fig. 3. The syzygy map takes a solution and lists its syzygy types in temporal order. Deleting the 'stutters' (e.g. $abaa \to ab$) makes this map well defined on free homotopy classes (see [3] Section 2 pgs. 3–6).

Theorem 1 implies the following: (the proof is identical to the proof in [3])

Corollary 1. *For the parallelogram problem, $\mathcal{P}$, the syzygy map from bounded parallelogram solutions to syzygy sequences is a bijection between the set of collision-free solutions, modulo symmetry and time-translation, and the set of bi-infinite non-stuttering collision-free syzygy sequences, modulo shift.*

The surface $\mathcal{C}$ consists of 12 invariant open disks, each disk corresponding to an ordering of the masses on the line (mod reversing the order due to a rotation by π). Restricting our attention to the closure of one of these invariant disks, $T \subset \mathcal{C}$ (e.g. $\{q : q_1 \le q_2 \le q_3 \le q_4\}$), we have:

Corollary 2. *For the collinear problem, $\mathcal{C}$, let $p, q \in \partial T \backslash$ {the two triple collision points} be two distinct points. Then there exists a unique solution connecting p to q, that is a solution $\gamma(t)$ with $\omega(\gamma) = p$ and $\alpha(\gamma) = q$.*

Open Questions: Does Corollary 2 hold when p and q are triple collisions? Does Corollary 1 hold for collision syzygy sequences? See Figs. 9, 10 for some collision orbits with matching syzygy sequences (giving some numerical evidence that the syzygy map is not 1–1 on collision orbits). Are there any solutions besides the rectangulars and rhomboids which have finite syzygy sequences?

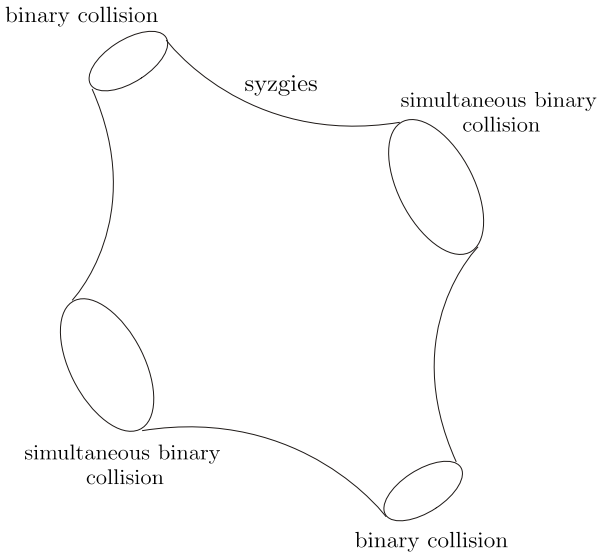

Fig. 2. The shirt.

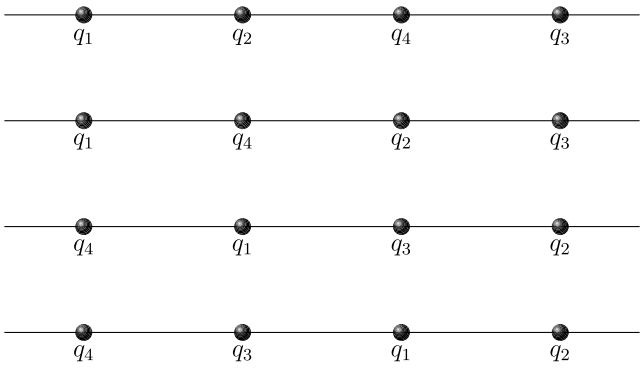

Fig. 3. Four syzygy types on $\mathcal{P}$.

2. Notations

A configuration for the planar 4-body problem will be written

$$q = (q_1, q_2, q_3, q_4),\ q_i \in \mathbb{C},$$

the configuration space is then

$$X = \mathbb{C}^4 \setminus \Delta$$

where $\Delta = \{q \in \mathbb{C}^4 : q_i = q_j, \text{ for some } i \neq j\}$ corresponds to collisions between two or more bodies. The dynamics for the inverse cube equal mass 4-body problem is the Hamiltonian flow of

$$H(q, p) = \frac{1}{2}|p|^2 - U(q)$$

for $(p, q) \in T^*X$ with symplectic form $\omega = \Re(\sum d\overline{p}_i \wedge dq_i)$ where

$$|p|^2 = \sum p_i \overline{p}_i$$

and

$$U = \sum_{i<j} |q_i - q_j|^{-2}$$

is the inverse cube potential.

We will form the quotient by the symmetry group G in stages. First we may reduce by translations simply by fixing the center of mass and the linear momentum. Hence we will work on

$$CM_0 := \{q \in X : \sum q_i = 0\}$$

with the condition

$$\sum p_i = 0$$

on the momentum. Note $CM_0 \cong \mathbb{C}^3 \setminus \{6 \text{ complex lines }\}$.

Since U is homogeneous of degree -2, the virial identity reads

$$\ddot{I} = 4H \tag{3}$$

along solutions, where

$$I = |q|^2.$$

Observe that for $H \neq 0$ solutions are either unbounded or end in total collision ($I = 0$). *Hence the energy zero case is the only interesting case with regard to finding periodic motions.*

The Jacobi–Maupertuis principle (see [9] pg. 247) states that the solutions to this inverse cube problem at this fixed energy level $H = 0$ are, up to reparametrization, geodesics of the metric

$$Uds^2_{Eucl} \tag{4}$$

where

$$ds^2_{Eucl} = \sum dq_i d\overline{q}_i$$

is the usual Euclidean metric restricted to CM_0.

Again, due to U's homogeneity of degree -2, the metric (4) is invariant under complex multiplication. Hence the Hopf map:

$$\pi_{Hopf} : CM_0 \setminus 0 \to \mathbb{C}P^2 \setminus P\Delta = Q$$

defined by mapping $q \in CM_0$ to the complex span of q pushes down (4) by submersion to induce a metric ds^2_{JM} on the quotient space which we call the Jacobi–Maupertuis metric (or JM-metric) on the reduced space. Here $P\Delta$ is the complex projectivization of $\Delta \cap \overline{CM_0}$. See [3,6,10,11], for more details about the Riemannian submersions in the reduction process.

Remark. In [3] these inverse cube ds^2_{JM} metrics are shown to be complete. The geodesics of ds^2_{JM} on Q lift to geodesics of (4) moving perpendicularly to the fibers $\mathbb{C}q$, which is equivalent to satisfying the conditions $\dot{I} = ds^2_{Eucl}(q, \dot{q}) = 0$ (or $I = const.$) and angular momentum $J = ds^2_{Eucl}(iq, \dot{q}) = 0$. From this quotient by scaling we can then always restrict ourselves to representatives in Q with $I = const. > 0$. Dynamically this choice is consistent with $H = 0$ and Eq. (3).

We now define the invariant surfaces corresponding to the parallelogram and collinear problems. We do so by using isometric involutions. Recall the fixed point sets of isometric involutions are always totally geodesic. Let

$$\Phi_{\mathcal{P}}(q_1, q_2, q_3, q_4) = -(q_3, q_4, q_1, q_2)$$

$$\Phi_{\mathcal{C}}(q_1, q_2, q_3, q_4) = (\overline{q}_1, \overline{q}_2, \overline{q}_3, \overline{q}_4)$$

and set

$$\mathcal{P} = \pi_{Hopf}(\text{Fix}\Phi_{\mathcal{P}}) \cong S^2 \setminus \{4 \text{ points}\}$$

$$\mathcal{C} = \pi_{Hopf}(\text{Fix}\Phi_{\mathcal{C}}) \cong \mathbb{R}P^2 \setminus RP\Delta,$$

(see Fig. 1). Here the $S^2 \setminus \{4pts.\} \cong \mathbb{C}P^1 \setminus \{4pts.\}$ and $RP\Delta$ is the real projectivization of $\Delta \cap \overline{CM_0}$.

3. Proof of results

The proof of Theorem 1 boils down to computing Gaussian curvatures of $\mathcal{P}$ and $\mathcal{C}$. Over $\mathcal{P}$, we follow the techniques of [10] using the nice coordinates from [7]. Over $\mathcal{C}$ we take convenient coordinates in which the computation reduces to checking the sign of a Laplacian.

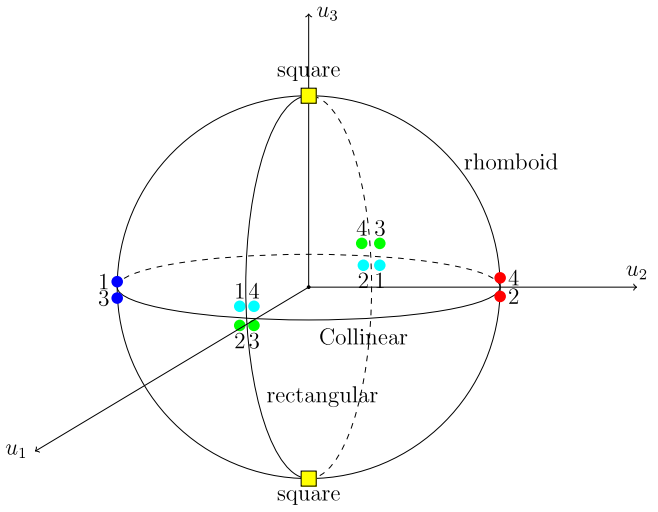

Fig. 4. The shape sphere or reduced space corresponding to parallelogram configuration in the case of equal masses. The equator corresponds to collinear parallelograms. There are two binary collisions and two simultaneous binary collisions on the equator. The rhombus and rectangles are great circles and these intersect in the poles, which corresponding to squares distinguished only by their orientation. See [7].

Proof of Theorem 1.

We will first compute the curvature over $\mathcal{P}$.

Consider the symmetry of the problem: $q_1 = -q_3$ and $q_2 = -q_4$. In this case the (negative) potential function has the following form

$$U = \frac{2}{r_{12}^2} + \frac{2}{r_{14}^2} + \frac{1}{r_{13}^2} + \frac{1}{r_{24}^2}. \tag{5}$$

Next we take the quotient by rotations. As in [7], consider Jacobi's coordinates and the Hopf map:

$$(q_1, q_2, q_3, q_4) \mapsto (q_2 - q_1, -q_2 - q_1) =: (z_1, z_2) \in \mathbb{C}^2,$$
$$(z_1, z_2) \mapsto \left(\frac{1}{2}\left(|z_1|^2 - |z_2|^2\right), \bar{z}_1 z_2\right) =: (u_1, u_2, u_3) \in \mathbb{R}^3.$$

Using the above formulas, it is immediate to see that ([11, Theorem 1])

$$I = |z_1|^2 + |z_2|^2 = 2\sqrt{u_1^2 + u_2^2 + u_3^2}, \qquad I = \text{constant}.$$

The following Lemma describes the relation between points of $\mathcal{P}$ and the mutual distances r_{ij} (see [7]):

Lemma 6. *For $u = (u_1, u_2, u_3) \in \mathcal{P}$, we have*

(1) $r_{12}^2 = |z_1|^2 = \frac{I}{2} + u_1$,
(2) $r_{14}^2 = |z_2|^2 = \frac{I}{2} - u_1$,
(3) $r_{13}^2 = |z_1 + z_2|^2 = I + 2u_2$,
(4) $r_{24}^2 = |z_1 - z_2|^2 = I - 2u_2$.

In particular, observe that $u_1 = 0$ if and only if the configuration is a rhombus, and $u_2 = 0$ if and only if the configuration is a rectangle. So, we have that on the north or south pole the configuration is a square. See Fig. 4.

We will use the following Lemma in our computations:

Lemma 7. *Let a surface be endowed with conformally related metrics ds^2 and $d\bar{s}^2 = U ds^2$. Then their curvatures K and $\overline{K}$ are related by*

$$U\overline{K} = K - \frac{1}{2}\Delta \log U$$

where the Laplacian Δ is with respect to the ds^2 metric.

From Eq. (5) and Lemma 6, the potential can be written as

$$U(u_1, u_2) = \frac{4}{I + 2u_1} + \frac{4}{I - 2u_1} + \frac{1}{I + 2u_2} + \frac{1}{I - 2u_2}, \qquad I = \text{constant}. \tag{8}$$

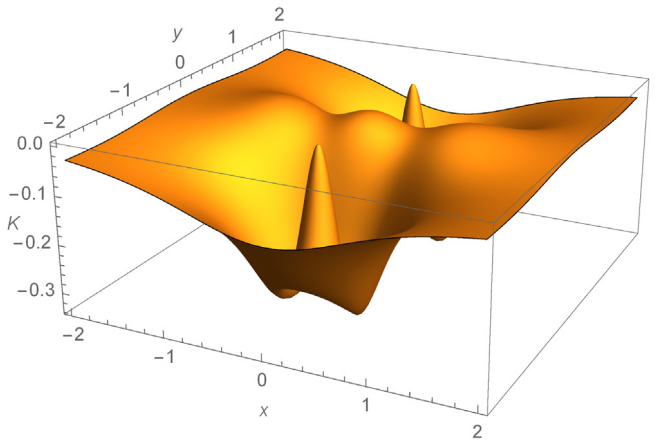

Fig. 5. Graph of the Gaussian curvature $K(x, y)$ of the surface $\mathcal{P}$ corresponding to configurations that are parallelograms.

Taking $I = 2$, we have $u_1^2 + u_2^2 + u_3^2 = 1$. As in [10], we use the stereographic projection from north pole $(0, 0, 1)$ given by

$$x = \frac{u_1}{1 - u_3}, \qquad y = \frac{u_2}{1 - u_3}, \tag{9}$$

we obtain $U(x, y) = (x^2 + y^2 + 1)f(x, y)$, where

$$f(x, y) = \frac{2}{(x + 1)^2 + y^2} + \frac{2}{(x - 1)^2 + y^2} + \frac{1}{2(x^2 + (y + 1)^2)} + \frac{1}{2(x^2 + (y - 1)^2)}.$$

We can also write the Jacobi–Maupertuis metric on the shape sphere as

$$ds_{JM}^2 = \frac{4U(x, y)}{(x^2 + y^2 + 1)^2}(dx^2 + dy^2) = \frac{4f(x, y)}{x^2 + y^2 + 1}(dx^2 + dy^2). \tag{10}$$

Write $\lambda(x, y) = \frac{4f(x,y)}{x^2+y^2+1}$. By Lemma 7, the Gaussian curvature of ds_{JM}^2 is given by

$$K(x, y) = -\frac{1}{2\lambda(x, y)} \Delta \log \lambda(x, y). \tag{11}$$

By a direct calculation we have

$$\Delta \log \lambda(x, y) = \frac{256(x^2 + y^2)}{[5 + 5x^4 - 6y^2 + 5y^4 + 2x^2(3 + 5y^2)]^2}. \tag{12}$$

Note that $\Delta \log \lambda(x, y) \geq 0$, and $\Delta \log \lambda(x, y) = 0$ if and only if $x = y = 0$. Therefore we conclude that K is negative on $\mathcal{P}$ except at the points corresponding to the square configurations.

Remark. As in [3], we consider the Gaussian curvature of $\mathcal{P}$ near the (simultaneous) binary collisions. In the same way as in [10], from Eqs. (11) and (12), we obtain

$$\lim_{(x,y)\to C} K(x, y) = 0,$$

where C is some (simultaneous) binary collision, see Fig. 5. It follows from this and completeness that the ends are asymptotic to Euclidean cylinders. In fact, if R_{ij} is the radius of the Euclidean cylinder when we approach the ij end, we have that (see [3, eq. 3.16] for explicit computations)

$$R_{13} = R_{24} = \frac{1}{\sqrt{2}}, \qquad \text{(binary collisions)},$$

and

$$R_{12} = R_{14} = 1, \quad \text{(simultaneous binary collisions)}.$$

Now we compute the Gaussian curvature over $\mathcal{C}$ and show it is negative.

Take the coordinates:

$$2\xi_1 = q_1 - q_2 - q_3 + q_4,\ \ 2\xi_2 = q_1 - q_2 + q_3 - q_4,$$

$$2\xi_3 = q_1 + q_2 - q_3 - q_4 \tag{13}$$

where we have

$$U = \sum_{1\le i<j\le 3} \frac{1}{|\xi_i - \xi_j|^2} + \frac{1}{|\xi_i + \xi_j|^2}$$

for $\xi_j = x_j + iy_j \in \mathbb{C}$ and $j = 1, 2, 3$.

Reducing the collinear configurations by dilations and rotations amounts to restricting the metric

$$U|_{\mathbb{R}^3} ds^2_{Eucl}$$

to the sphere $I = 1$ (with antipodal points identified).

That is in the usual spherical coordinates ($I = \rho^2$) we wish to compute the curvature, K_C, of

$$\hat{U}I(d\phi^2 + \cos^2\phi d\theta^2)$$

where $\hat{U} := U|_{\mathbb{R}^3}$. Set $u = \hat{U}I = U|_{S^2}$.

By Lemma 7:

$$uK_C = 1 - \frac{1}{2}\Delta_{S^2} \log u$$

where Δ_{S^2} is the Laplacian on the sphere.

As:

$$\Delta_{S^2} \log u = (\Delta \log \rho^2 \hat{U})|_{S^2} = (\Delta \log \hat{U})|_{S^2} + 2$$

where Δ is the standard Laplacian on $\mathbb{R}^3$, we see $K_C < 0$ is equivalent to $(\Delta \log \hat{U})|_{S^2} > 0$.

So it suffices to show that $\Delta \log \hat{U} > 0$.

It is easy to check that when $V \subset \mathbb{C}^M$ is an affine subvariety and $f : \mathbb{C}^M \setminus V \to \mathbb{C}^{M'} \setminus 0$ is holomorphic that $\sum_{j=1}^{M} \frac{\partial^2 \log \|f\|^2}{\partial z_j \partial \bar{z}_j} \ge 0$. Moreover, the inequality is strict when $M' > 1$ and $\frac{\partial f}{\partial z_j} \ne \lambda f$ for any $\lambda \in \mathbb{C}$ and some $j \in \{1, \dots, M\}$.

Hence setting $f^-_{ij}(\xi_1, \xi_2, \xi_3) = 1/(\xi_i - \xi_j)^2, f^+_{ij}(\xi_1, \xi_2, \xi_3) = 1/(\xi_1 + \xi_j)^2$ and $\phi = \log U = \log \|f\|^2$ we have

$$\Delta_{\mathbb{C}^3}\phi := \sum_{j=1}^{3} \frac{\partial^2 \phi}{\partial x_j^2} + \frac{\partial^2 \phi}{\partial y_j^2} > 0.$$

Take $x = (x_1, x_2, x_3)$ and $y = (y_1, y_2, y_3)$. The symmetry $\phi(x, y) = \phi(y, x)$ implies

$$\frac{\partial^k \phi}{\partial x_j^k}(x, y) = \frac{\partial^k \phi}{\partial y_j^k}(y, x).$$

Now since $\phi(x, 0) = \phi(0, x) = \phi(x, x) + const.$ we have

$$2\left(\frac{\partial^2 \phi}{\partial x_j^2}(x, x) + \frac{\partial^2 \phi}{\partial y_j^2}(x, x)\right) = \frac{\partial^2 \phi}{\partial x_j^2}(x, 0)$$

and so

$$\Delta \log \hat{U} = 2\Delta_{\mathbb{C}^3}\phi(x, x) > 0$$

as desired. □

Proof of Corollary 2. Continue with the coordinates $\xi_j = x_j + iy_j$ of Eq. (13). After the spherical projection:

$$u = \frac{x_1 + x_2}{1 - x_3}, v = \frac{x_1 - x_2}{1 - x_3}$$

of the $I = 1$ sphere, our metric $U(\sum dx_i^2)|_{S^2}$ becomes $\frac{\lambda}{2}(du^2 + dv^2)$ with:

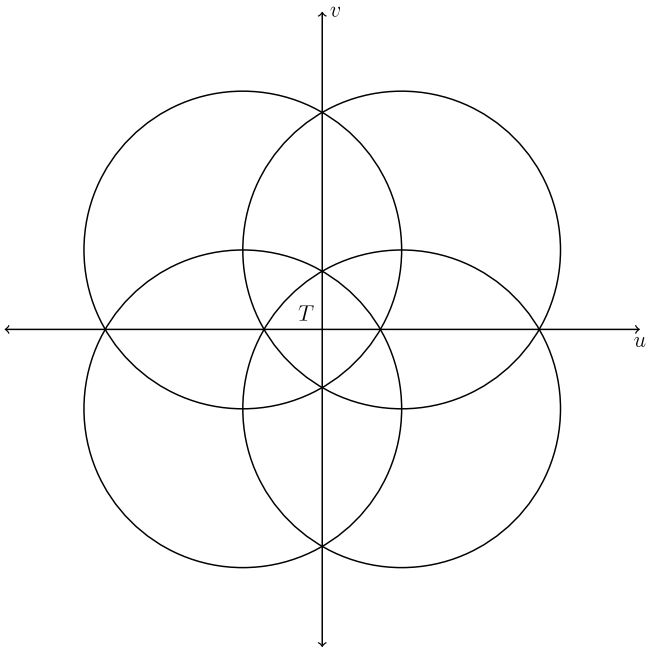

Fig. 6. The region T we are focusing on in u, v coordinates.

$$\lambda = \frac{1}{u^2} + \frac{1}{v^2} + \frac{16}{((u-1)^2+(v-1)^2-4)^2} + \frac{16}{((u+1)^2+(v+1)^2-4)^2} + \frac{16}{((u+1)^2+(v-1)^2-4)^2} + \frac{16}{((u-1)^2+(v+1)^2-4)^2}.$$

The $\mathbb{R}P^2$ of collinear shapes is divided into $12 = 4!/2$ open domains by the collision locus. All of these domains are isometric and resemble triangles, the interiors of which are specified by an ordering of the masses on the line (mod an overall flip due to a rotation by π). See Fig. 6. We focus on one such domain T corresponding to the ordering $q_1 \leq q_2 \leq q_3 \leq q_4$. Here the boundary in u, v coordinates translates to:

$$u = 0 \iff q_1 = q_2$$

$$v = 0 \iff q_3 = q_4$$

$$w = (u-1)^2 + (v+1)^2 - 4 = 0 \iff q_2 = q_3.$$

Near a binary collision point interior to T (for example near $q_1 = q_2$ in a region $0 < -u \ll 1$ and $v, -w \geq \delta > 0$) the metric takes the form

$$(\frac{1}{2u^2} + O(1))(du^2 + dv^2). \tag{14}$$

Near the simultaneous binary collision, i.e. in the region $0 < -u, v \ll 1$, through the change of variable $u + iv = z \mapsto z^2$, the metric takes the same form as Eq. (14).

Fix our attention on unit speed geodesics and note that by Eq. (14) above if a geodesic γ passes sufficiently close to the boundary it behaves as a geodesic in the hyperbolic plane, for instance $\alpha(\gamma) \cap \partial T$ must be a point, see Fig. 7 and the Appendix.

Fix some $q \in \partial T \backslash \{\text{triple collisions}\}$ and $p \in \partial T \setminus \{q\}$. We first show the existence of a geodesic from p to q.

Near q (by Eq. (14)) we have that every geodesic γ with $\omega(\gamma)$ sufficiently near p and $\alpha(\gamma)$ near q intersects some compact set I, see Fig. 8.

Next take a sequence of points $q_i \in T^o$ with $q_i \to q$ and a sequence of points $p_i \in T^o$ with $p_i \to p$. Let γ_i be the unique geodesic from p_i to q_i. Then for i large enough all such geodesics intersect I in some point $x_i = \gamma_i(t_i)$. Let $v_i = \dot{\gamma}_i(t_i)$. Now due to the compactness, $(x_i, v_i) \to (x, v) \in I \times \mathbb{R}^2$ and the geodesic with this initial condition $\gamma_{(x,v)}$ goes from p to q.

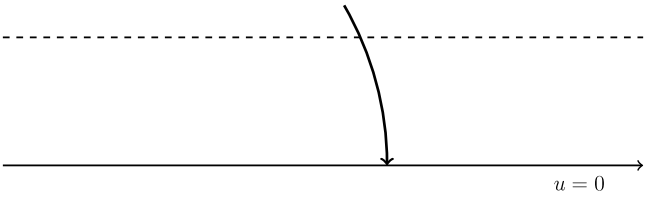

Fig. 7. Sufficiently near the boundary geodesics behave as in the upper half plane. See Appendix for details.

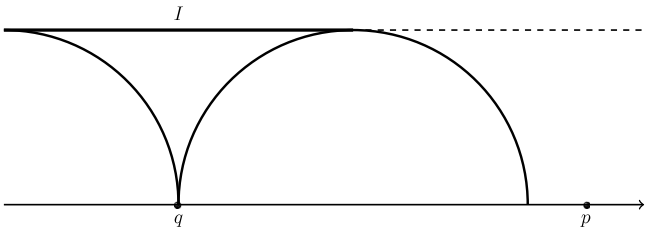

Fig. 8. The compact set I. See Appendix for details.

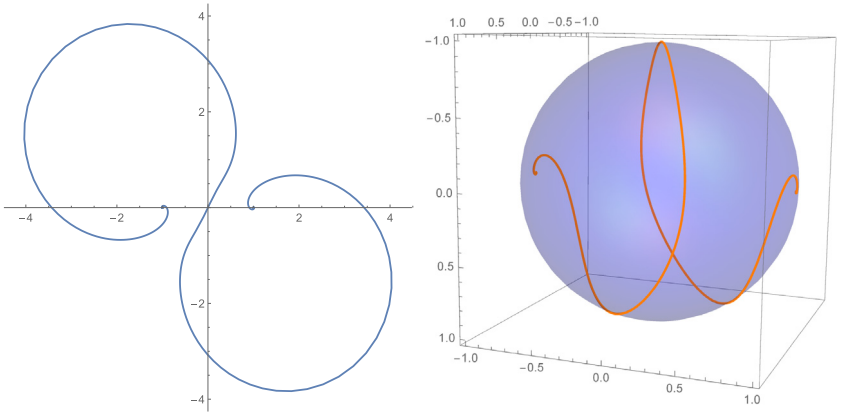

Fig. 9. A distinct collision solution seen from the (x, y)-plane (*on the left*) and in the shape sphere (*on the right*). In this case the collisions are simultaneous binary collisions.

For uniqueness, note that when we have both $p, q \in \partial T \backslash \{\text{triple collisions}\}$ then the angles at the boundary between any two geodesics from p to q are zero (see Appendix). So if there were two such geodesics bounding a region R, the Gauss–Bonnet theorem yields

$$2\pi = \int_R K \, dA + \int_{\partial R} \kappa_g \, ds = \int_R K dA + \pi + \pi,$$

which is impossible by the negative curvature. Hence in this case such a geodesic is unique. □

Remark. Due to the covering of the exponential map, every geodesic passes sufficiently close to the boundary and hence is characterized uniquely by the points $\alpha(\gamma)$, $\omega(\gamma)$ (except possibly for geodesics beginning or ending in triple collision). The dynamics here on $\mathcal{C}$ are an attractive case of the *integrable* Calogero–Moser system.

Acknowledgments

We would like to thank Richard Montgomery for his advice and guidance with the writing process and conversations on the perturbed metrics. Also we thank Rick Moeckel who posed the question leading to Corollary 2, and Gabriel Martins for conversations on the parallelogram space.

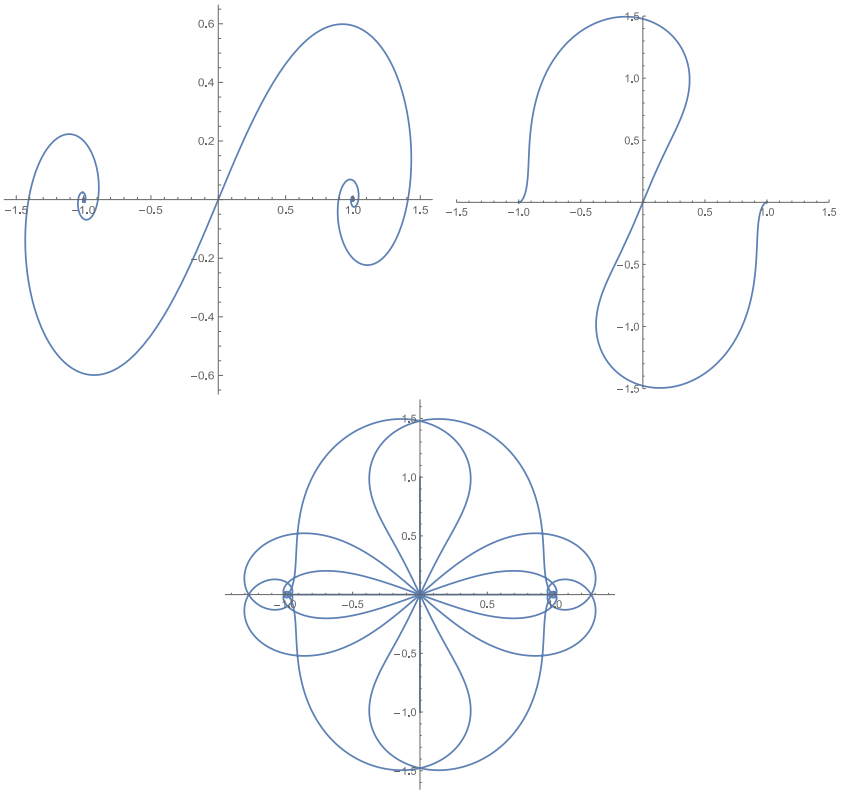

Fig. 10. Solutions with collision seen from the (x, y)-plane. Note that all these solutions pass through a square configuration, corresponding to the south pole in the shape sphere.

Appendix. On a metric of the form of Eq. (14)

Here we establish Figs. 7, 8 for the behavior of Eq. (14) near the boundary $\partial T \setminus \{\text{triple collisions}\}$ that were used in the proof of Corollary 2.

Our metric Eq. (14) has the form:

$$(\frac{1}{y^2} + f(x, y))(dx^2 + dy^2) = \frac{\phi}{y^2}(dx^2 + dy^2)$$

on the upper half plane $z = x + iy, y > 0$ where $\phi, \frac{1}{\phi} \in O(1), \phi_x \in O(y^2)$ and $\phi_y \in O(y)$ as $y \to 0$. Recasting in Hamiltonian form, that is with

$$H = \frac{y^2}{2\phi}(p_x^2 + p_y^2)$$

the equations of motion for $H = 1$ (so $yp_x, yp_y \in O(1)$) read:

$$\dot{x} = \frac{y^2}{\phi}p_x, \dot{y} = \frac{y^2}{\phi}p_y,$$

$$\dot{p}_x = \frac{\phi_x}{\phi}, \dot{p}_y = -\frac{2}{y} + \frac{\phi_y}{\phi}.$$

In particular for y sufficiently small we have $\dot{p}_y < 0$ so that entering such a sufficiently near region of the boundary ($p_y(0) < 0 \Rightarrow p_y(t) < 0$) implies $\dot{y} < 0$ and $y \to 0$ as $t \to \infty$ (see Fig. 7). Moreover near the boundary we may parametrize geodesics by y as they approach or leave the boundary.

Parametrizing now by y and letting $'$ denote $\frac{d}{dy}$ we have:

$$p_y p_y' = -\frac{2}{y^3} + O(\frac{1}{y}) \Rightarrow p_y^2 = \frac{1}{y^2} + O(\log y) + c_y$$

and

$$p_x' = O(\frac{1}{p_y}) = O(y) \Rightarrow p_x = O(y^2) + c_x$$

where c_x and c_y are constants. In particular, $p_y \to \infty$ and $p_x \to c_x$ as $y \to 0$ so that $\theta = \arctan(\dot{y}/\dot{x}) = \arctan(p_y/p_x) \to \pi/2$ i.e. all orbits intersect the boundary perpendicularly.

Take an ε small enough so that the above observations hold over $y \leq \varepsilon$.

Now we direct our attention towards establishing Fig. 8.

Reparameterize by y, to obtain

$$|\frac{dx}{dy}| = |\frac{p_x}{p_y}| = \frac{y|p_x|}{\sqrt{1 + y^2 O(\log(y)) + c_y y^2}} = \frac{y|p_x|}{1 + O(y)}.$$

In particular as $p_x = O(y^2) + c_x$, any orbit entering $y \leq \varepsilon$ with an initial $|p_x(\varepsilon)| = \delta$ at the instant $y = \varepsilon$ has

$$|p_x| \leq \delta + O(\varepsilon^2)$$

over the rest of its fall so that

$$|x'| \leq c_1 y(\delta + O(\varepsilon^2))$$

and

$$|x(\varepsilon) - x(y)| \leq c_1 \varepsilon^2 \delta + O(\varepsilon^4)$$

for some constant c_1.

Moreover by energy conservation, $H = 1$, we have $\delta = |p_x(\varepsilon)| \leq \frac{\sqrt{2\phi}}{\varepsilon}$, so that

$$\delta \leq \frac{c_2}{\varepsilon}$$

for some constant c_2.

Hence any geodesic entering $y \leq \varepsilon$ at $x(\varepsilon) + i\varepsilon$ will hit the boundary at a point $x(0)$ with

$$|x(\varepsilon) - x(0)| \leq c\varepsilon$$

for some constant c. Likewise by reversing the time a geodesic leaving the region $y \leq \varepsilon$ at $x(\varepsilon) + i\varepsilon$ will have come from a boundary point $x(0) = x(\varepsilon) + O(\varepsilon)$.

Divide those geodesics coming into q into two classes:

1. those that do not intersect $y = \varepsilon$,
2. those that intersect $y = \varepsilon$.

For the geodesics of class 1, we have by $\dot{p}_y < 0$ that there is a unique maximum attained at $y = M < \varepsilon$. Now our estimates above imply we intersect the boundary again a distance at most $2cM < 2c\varepsilon$ from q.

Consider geodesics of class 2 intersecting $y = \varepsilon$ at $q + x(\varepsilon) + i\varepsilon$. Then by the above, once $|x(\varepsilon)| > c\varepsilon$ such a geodesic cannot reach q, hence all such geodesics of class 2 intersect the compact set $\{q + x + iy : -c\varepsilon \leq x \leq c\varepsilon, y = \varepsilon\}$.

In particular we can establish Fig. 8 by choosing ε small enough that p does not lie within $c\varepsilon$ of q.

References

[1] H. Poincaré, Sur les solutions périodiques et le principe de moindre action, C. R. Hebd. Seances Acad. Sci. Paris 123 (1896) 915–918.
[2] W. Gordon, Conservative dynamical systems involving strong forces, Trans. Amer. Math. Soc. 204 (1975) 113–135.
[3] R. Montgomery, Hyperbolic pants fit a three-body problem, Erg. Th. Dyn. Syst. 25 (2005) 921–947.
[4] Toshiaki Fujiwara, Hiroshi Fukuda, Hiroshi Ozaki, Tetsuya Taniguchi, Saari's homographic conjecture for general masses in planar three-body problem under newton potential and a strong force potential, J. Phys. A 48 (2015) 265–205.
[5] G. Roberts, Some counterexamples to a generalized Saari's conjecture, Trans. Amer. Math. Soc. 358 (1) (2005) 251–266.
[6] C. Jackman, R. Montgomery, No hyperbolic pants for the 4-body problem with strong potential, Pacific J. Math. 280 (2) (2016) 401–410.
[7] KC. Chen, Action minimizing orbits in the parallelogram four-body problem with equal masses, Arch. Ration. Mech. Anal. 158 (4) (2001) 293–318.
[8] A. Albouy, On the force fields which are homogeneous of degree -3, in: M. Corbera, J. Cors, J. Llibre, A. Korobeinikov (Eds.), Extended Abstracts Spring 2014, in: Trends in Mathematics, vol. 4, Birkhäuser, Cham, 2015.
[9] V.I. Arnold, Mathematical Methods of Classical Mechanics, second ed., Springer, 1997.
[10] M. Alvarez-Ramírez, A. García, J. Meléndez, J. Guadalupe Reyes-Victoria, The three-body problem with equal masses via the hyperbolic pants and equivariant Riemannian geometry, J. Math. Phys. 58 (8) (2017).
[11] R. Montgomery, The three body problem and the shape sphere, Amer. Math. Monthly 122 (4) (2015) 299–321.